Propagation of ultrashort pulses in multimode fiber in space and time

Rostislav Rokitski and Shaya Fainman
University of California, San Diego, La Jolla, CA 92093
rokitski@ucsd.edeu

http://topaz.ucsd.edu

Abstract: We perform 3D cross-correlation measurements of the optical field distribution resulting from an ultrashort pulse propagating in 6 meters of multimode fiber. Spatial amplitude and phase distributions of the optical field at the output of the fiber are measured using a time-gated spatial heterodyne interferometer as a function of time delay between the signal and the reference optical fields. We show that the measured signal represents an approximation to the optical impulse response of the multimode fiber.

OCIS codes: (320.0320) Ultrafast optics, (060.2310) Fiber optics, (100.4550) Optical correlators

References and Links

1. A. Yariv, "Three-dimensional pictorial transmission in fibers," Appl. Phys. Lett. **28**, 88 (1976)
2. G.J. Dunning, R.C. Lind, "Demonstration of image transmission through fibers by optical phase conjugation," Opt. Lett. **7**, 558, (1982)
3. S.E. Miller, N.J. Locust, "Mode detection and delay equalization in multimode optical fiber transmission systems," U.S. Patent 3,777,150 (1973)
4. Teiji Uchida, Atsufumi Ueki, "Mode separator and delay equalizer for multimode optical fiber transmission systems," U.S. Patent 4,050,782 (1977)
5. K.M. Patel, S.E. Ralph, "Enhanced multimode fiber link performance using a spatially resolved receiver," IEEE Phot. Tech. Lett. **14**, 393 (2002)
6. X. Zhao, F.S. Choa, "Demonstration of 10-Gb/s transmissions over a 1.5-km-long multimode fiber using equalization techniques," IEEE Phot. Tech. Lett. **14**, 1187 (2002)
7. H.R. Stuart, "Dispersive Multiplexing in Multimode Optical Fiber," Science **289**, 281 (2000)
8. G.J. Foschini and M.J. Gans, "On Limits of Wireless Communications in a Fading Environment when Using Multiple Antennas," Wireless Personal Communications **6**, 311, (1998)
9. R. Rokitski, P. C. Sun, Y. Fainman, **"**Study of spatial-temporal characteristics of optical fiber based on ultrashort-pulse interferometry," Opt. Lett. **26**, 1125 (2001)
10. B. Järne, *Digital Image Processing* (Springer-Verlag, Berlin, 1995)
11. D.C. Ghiglia, M.D. Pritt, *Two-dimensional Phase Unwrapping* (John Wiley & Sons, New York, 1998)

1. Introduction

Multimode optical fibers have great potential for information transmission. In addition to the wavelength degree of freedom currently utilized in single-mode fibers, multimode fibers possess two additional spatial coordinates that can be used as additional degrees of freedom to increase the channel capacity for optical communication. Many groups tried to utilize this potential for image transmission through a single multimode fiber [1,2] using optical wavefront conjugation, position-sensitive optical signal detection [3-5] and equalization methods [6,7], however the complexity of mode separation setups and mode coupling due to fiber inhomogeneities still limit full utilization of multimode fiber potential. One of the major difficulties, preventing efficient information transmission through a multimode fiber, comes

#2174 - $15.00 US Received February 03, 2003; Revised June 12, 2003

from phase randomization between different spatial modes, acquired during propagation to the output of the fiber, and results in temporal and spatial speckle. Recent advances in radio frequency communication in multipath environments [8] suggest that the multimode signal spread can be compensated by using a multiple detector array with an adaptive signal equalizer. Implementation of such a system in the optical domain requires knowledge of the complex amplitude of the optical waves at the receiver, since these systems rely on the coherent addition of the signals coming from multiple detectors. Design and operation of such a detection system would benefit from better understanding of how the optical signal propagates in multimode fibers in space and time. In this manuscript we employ a space-time characterization technique, based on spatial heterodyne interferometry [9] to analyze propagation of optical pulses in multimode fibers in space and time.

2. Measurement technique and setup

We consider a scenario when an ultrashort optical pulse, carrying two-dimensional information, is launched into a multimode fiber. Guiding modes of the fiber, carrying spatial information, propagate with different velocities and each mode acquires some random shift with respect to initial phase. Therefore the optical field at the output of the fiber has unknown temporal and spatial characteristics, depending on the fiber length and random phase distribution between the spatial modes, caused by environment and imperfection of the geometric boundaries. In our approach an unknown optical field $E_1(\vec{r},t)$ at the output of the multimode fiber is characterized in space and time using time-gating reference field $E_2(\vec{r},t)$. These two optical fields, carrying a signal and an ultrashort reference pulse are superimposed at an angle θ with respect to each other and with a relative time delay τ on the surface of the photodetector (See Fig. 1). The interference pattern of the two fields is sampled in space and integrated in time using a CCD camera for different time delays τ. After performing a spatial discrete Fourier transform (DFT) of the sampled detected interference pattern and applying bandpass filtering in the spatial frequency domain, we obtain sampled spatial amplitude and phase distribution of the optical field at the output of the multimode fiber. In our experiments the wave vector of the signal pulse is normal to the observation plane (i.e., CCD), while the wave vector of the reference pulse makes an angle θ with the normal (see Fig. 1).

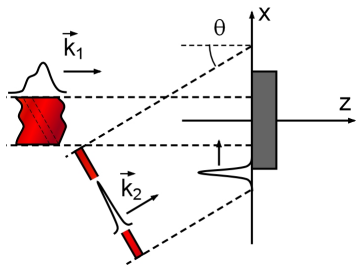

Fig. 1. Formation of the interference pattern between short pulses on the surface of CCD.

We assume that the signal field is imaged from the output of the fiber onto the CCD using a 4f imaging system, while a collimated Gaussian beam is used as a reference. The signal pulse and the reference pulse complex fields can be represented as

$$E_1(\vec{r},t) = U(\vec{r},t)\exp[\,j(\omega t + \phi(\vec{r},t) - \vec{k}_1 \cdot \vec{r})]$$
$$E_2(\vec{r},t) = p(\vec{r},t+\tau)\exp[\,j(\omega(t+\tau) - \vec{k}_2 \cdot \vec{r})] \quad (1)$$

#2174 - $15.00 US Received February 03, 2003; Revised June 12, 2003

where $p(\vec{r},t) = p(t-\vec{r}/c)$ is the reference pulse envelope, $\vec{k}_1, \vec{k}_2$ are the wave vectors of the signal and the reference pulses, respectively, ω is the center frequency of the pulse; $U(\vec{r},t)$ and $\phi(\vec{r},t)$ are amplitude and phase of the signal field. For simplicity we consider only one polarization of the interfering fields and assume that the reference pulse has a plane wavefront. Also the amplitude of the reference is assumed to be Gaussian, while the signal pulse has unknown spatial amplitude $U(\vec{r},t)$ and phase $\phi(\vec{r},t)$ distributions. Time dependence of the signal phase takes into account chromatic dispersion effects inside the fiber. The interference pattern exists on the surface of CCD only when two fields overlap in time. Because the reference pulse makes angle θ with detector's surface normal, its pulse front scans through the detector's aperture with phase velocity $c/\sin\theta$, where c is the speed of light in vacuum. Therefore, the interference pattern acquires temporal delay of $L\sin\theta/c$ along the path of the reference pulse on the detector surface, where L is size of the CCD in the direction of propagation of the reference. The fraction of the signal pulse, contributing to the observed interference pattern is shown by dashed lines in Fig. 1.

Total intensity of the interference pattern, detected by a CCD at the location $z = z_0$ is

$$\begin{aligned} I(\vec{r},t) &= \int_0^T \left|E_1(\vec{r},t) + E_2(\vec{r},t)\right|^2 dt \\ &= \int_0^T \left[\left|U(x,y,t)\right|^2 + \left|p(x,y,t+\tau)\right|^2 + U(x,y,t)\,p(x,y,t+\tau)\cos(\omega\tau + xk_{2x} + yk_{2y} + \phi(x,y,t))\right] dt \end{aligned} \tag{2}$$

where T is the integration time of the camera photodetectors, τ is the relative time delay between the signal and the reference pulse and k_{2x}, k_{2y} represent projections of the reference wave vector $\vec{k}_2$ on axes x and y. Dependence on z is omitted in all the functions since we fix the observation plane at $z = z_0$. First two terms under the integral result in a slowly varying background image, while the third term is the interference term between the signal and the reference fields carried by a spatial beating with spatial frequency $\vec{k}_2 = \{k_{2x}, k_{2y}\}$ in the observation plane $\{x, y\}$. In addition to temporal integration, the camera performs spatial sampling of the interference pattern, leading to a convolution of the observed intensity distribution with corresponding optical transfer function, defined by pixel's geometry [10]. This usually can be treated as additional lowpass filtering of the signal in the spatial frequency domain with sinc-shaped linear filter. For simplicity we leave these effects, out of our analysis.

We separate desired time-gated beat term in spatial frequency domain using a bandpass filter, centered at the positive spatial carrier frequency $\{k_{2x}, k_{2y}\}$. Filtered spatial spectrum is then shifted to the origin of the spatial frequency plane to cancel linear phase term $xk_{2x} + yk_{2y}$ in the space domain. Inverse Fourier transformation back to space domain gives an estimated signal field at time τ as a convolution of the imaged complex optical field from the output of the fiber with the envelope of the ultrashort reference pulse:

$$U_{est}(x,y,\tau) = \int_0^T U(x,y,t)\,p(x,y,t+\tau)\exp[\,j(\omega\tau + \phi(x,y,t))]\,dt \tag{3}$$

If the reference pulse is much shorter than the signal pulse and can be approximated by a delta function in the propagation direction $\vec{k}_2$ (see Fig. 1) producing in xy plane $p(x,y,t) \approx \delta(t - x\cos\hat{\theta}/c - y\sin\hat{\theta}/c)$, one would get the estimated signal field as

$$U_{est}(x,y,\tau) \approx \tilde{U}(x,y,\tau)\exp[\,j(\omega\tau + \tilde{\phi}(x,y,\tau))]\,, \tag{4}$$

where $\hat{\theta}$ is the angle between the x axis and the projection of $\vec{k}_2$ on the xy plane, tilde shows that the signal field is expressed in the coordinate system, rotated in xy plane around the origin by angle $\hat{\theta}$. Therefore, the estimated optical field distribution is directly related to the imaged optical field at the output of the fiber through the coordinate transformation:

#2174 - $15.00 US Received February 03, 2003; Revised June 12, 2003

$\{x, y, \tau\} \rightarrow \{x\cos\hat{\theta} - y\sin\hat{\theta}, x\sin\hat{\theta} + y\cos\hat{\theta}, \tau\}$. The reference pulse width defines resolution of the signal measurement in time domain.

Transform-limited short pulses with autocorrelation FWHM 180 fs, central wavelength 830 nm and optical bandwidth 8.4 nm are obtained from a Ti:Sapphire mode-locked laser (Coherent's "Mira 900"), operating at TEM_{00} spatial mode. The laser produces a stream of short pulses with repetition rate 76 MHz.

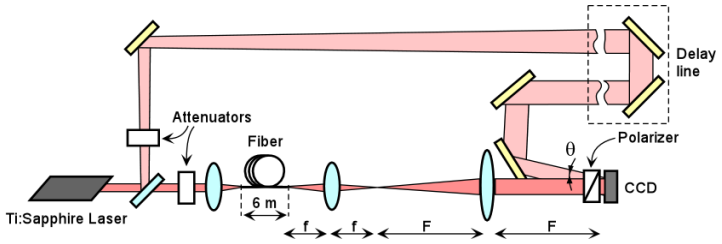

Fig. 2. Optical setup for time-gating spatial heterodyne measurements

One arm of the interferometer contains 6 meters of multimode optical fiber (50/125 Draka graded index fiber, optimized for 850 nm). Coupling of the pulse into the multimode fiber is performed using a 5x microscope objective. The second arm of the interferometer carries a reference pulse, derived from the same pulse stream, however separated from the signal stream by two periods (~25 ns). Reference field is produced by diffraction of the laser output in free space over the distance 4 m. The output of the fiber is imaged using a 4f system with magnification factor 100 onto the surface of the digital CCD camera with 10 bit intensity quantization, where it is combined with the beam from the reference arm of the interferometer. The angle of incidence of the reference beam is adjusted by monitoring interference pattern in the spatial Fourier transform domain. Spatial mode size of the reference beam in the detection plane was ~10 times larger than the signal mode size. Small spatial variation of the reference field amplitude and phase is taken into account by normalization during data processing. We achieve largest spatial frequency bandwidth, equal to inverse of one half of the resolution of the CCD, and largest signal/background separation in spatial frequency domain by placing the spatial carrier frequency in the center of one of the four quadrants in the spatial Fourier transform domain (the direction of the spatial frequency carrier is along the CCD diagonal). Temporal scanning of the fiber output is performed using a delay line with submicron resolution in the reference arm of the interferometer. Total scanning range of the delay line was ~175 ps. Variable optical attenuator is used to optimize visibility of the interference pattern. In our setup the signal pulse does not experience large depolarization effects due to short propagation distance; however the polarizations state of the field at the output of the fiber requires adjustment. We align polarization states of the two interfering beams using a Glan-Thomson polarizer in front of the CCD camera. Integration time of the camera was in the range of ~65-350 μs. During this time more than 5000 ultrashort pulse pairs produce interference patterns, integrated by the camera.

3. Experimental results

Interference pattern was measured by the CCD camera for a wide range of delays (0-175 ps). A typical sample of the measured interference pattern is shown in Fig. 3(a) together with the corresponding spatial spectrum (see Fig. 3(b)) in logarithmic grayscale. During the measurements the interference pattern was stable in time and we did not observe large motion of the interference fringes, caused by environmental changes, on the timeframe of several seconds. Since the camera integration time was on the order of several hundreds of microseconds, we conclude that the contrast ratio of the pattern was affected mostly by the

#2174 - $15.00 US Received February 03, 2003; Revised June 12, 2003

signal pulse spreading and not affected by relative phase randomization between the arms of interferometer, caused by environment changes. To obtain the estimate of the signal amplitude and phase given by Eq. (4), spatial spectrum of the interference pattern was at first shifted to the origin by the spatial carrier frequency $\{k_{2x}, k_{2y}\}$, which was determined from the spectrum as a center of mass of the high-frequency region of the spectrum.

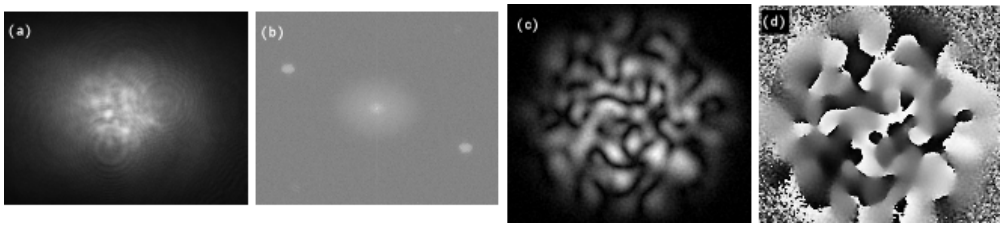

Fig. 3. (a) Observed interference pattern; (b) spatial spectrum of the interference pattern, shown in logarithmic grayscale; (c) reconstructed amplitude distribution of the signal field; (d) reconstructed spatial phase distribution of the signal field.

Then we applied 2D lowpass filter with Blackman window to perform filtering in the spatial spectrum domain, to obtain the sum of Fourier transformed estimates of the complex field U_{est}, represented by Eq. (3). The summation operation was performed by the CCD camera over the integration time window and included over 5000 optical pulses. Approximating the reference pulse by the δ-function we can use Eq. (4). Since the environmental changes had negligible effect on the interference pattern during a single measurement, we assume that our estimated U_{est} represents time average of the optical amplitude at the output of the fiber. Corresponding amplitude and wrapped phase distributions, normalized by the reference amplitude and phase profiles, are presented in Fig. 3(c) and Fig. 3(d). Since the spatial phase distribution was derived as an argument of the reconstructed complex field as given in Eq. (4), it has the values wrapped around 2π. Some applications (for example, when our technique is used for profilometry or optical coherence tomography) can benefit from unwrapped spatial phase distributions that can be obtained using one of well-known 2D phase unwrapping techniques [11].

Spatial amplitude and phase distributions of the signal field have been measured for several positions of the delay line. We present the amplitude of the optical field as a movie, where each frame of the movie corresponds to a different position of the delay line. Total range of delays, presented in the movie is τ = 20-35 ps. Total optical power at the output of the fiber, calculated in the spatial frequency domain, is shown in Fig. 4 as a function of time delay τ.

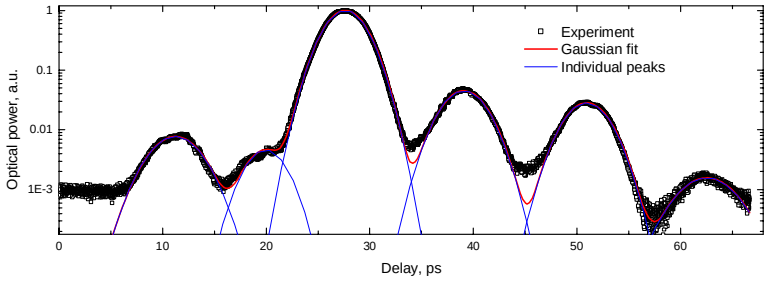

Fig. 4. Total optical power at the observation plane as a function of time delay τ.

The peak with highest intensity, centered at 27 ps delay corresponds to the true impulse response of the fiber, while the other peaks with lower intensity originate from secondary

#2174 - $15.00 US
Received February 03, 2003; Revised June 12, 2003

reflections of the ultrashort pulse in our optical setup (CCD's cover glass, etc.). By removing the cover glass from the CCD chip these secondary peaks can be eliminated from the measured impulse response. We will limit our observation window to 15 ps range and not consider the secondary reflections. The largest peak represents a cross-correlation of the signal pulse with the reference short pulse and can be considered as an approximate time domain optical power impulse response of the multimode fiber. It has almost Gaussian shape with RMS width of ~3.5 ps.

We analyzed optical impulse response at the individual pixel locations in the observation plane. The results are shown in the Figs. 5(a) and (b) together with the total power, integrated over the area of CCD. Impulse responses of the individual pixels consist of several narrow peaks with RMS width ~0.5-0.9 ps, concentrated in several locations. The distribution of peak centers and the amplitudes varies from pixel to pixel and in the case of large distance between the pixels, the shapes of the corresponding impulse response functions have very little in common, since the optical energy arrives at the different pixels through the different sets of modes of the fiber. The impulse response functions measured at the adjacent pixel locations have very similar shape, as shown in Fig. 5(b).

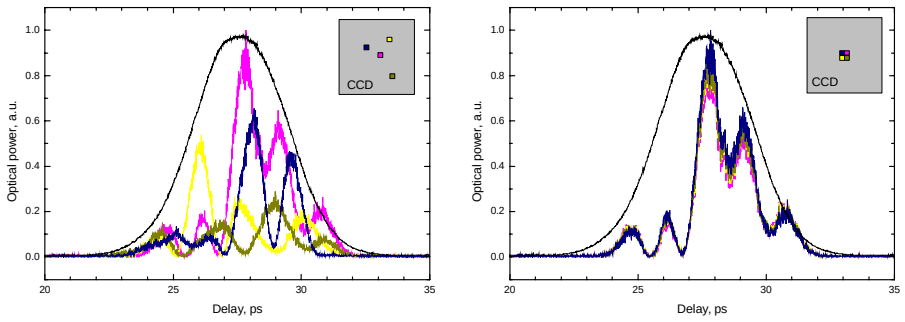

Fig. 5. Optical power impulse response of the multimode fiber: a) impulse response of 4 pixels randomly selected across the aperture of the fiber b) impulse response of 4 adjacent pixels in the center of the aperture. Total optical power is shown by black line in both graphs. Lines with different colors correspond to optical impulse response at the locations of individual pixels. Location of the pixels inside the CCD matrix is shown approximately by color squares in the top right corner of the graphs.

4. Conclusion

We characterized in space and time the propagation of an ultrashort pulse in a multimode optical fiber using time-gated spatial heterodyne interferometry. The optical field amplitude and phase at the output of the fiber was estimated as a function of delay. For our fiber length and coupling conditions the output optical signal, integrated over the detector area consists of a single broad Gaussian pulse, resulting in a total group delay of ~3.5 ps. The impulse response measured at individual pixel locations contains a series of narrow pulses.

Acknowledgements

This work was supported by NSF, AMCC, DARPA and AFOSR. We would like to thank Draka Comteq for providing new generation multimode optical fiber used in our experiment.